Electronic Supplementary Material (ESI) for Green Chemistry.

# Supplementary Information

## Ultra-low temperature carbon (di)oxide hydrogenation catalyzed by hybrid ruthenium-nickel nanocatalysts: towards sustainable methane production

Tomasz Siudyga, Maciej Kapkowski, Piotr Bartczak, Maciej Zubko, Jacek Szade, Katarzyna Balin, Sylvain Antoniotti*, Jaroslaw Polanski (ORCID 0000-0001-7361-2671) *

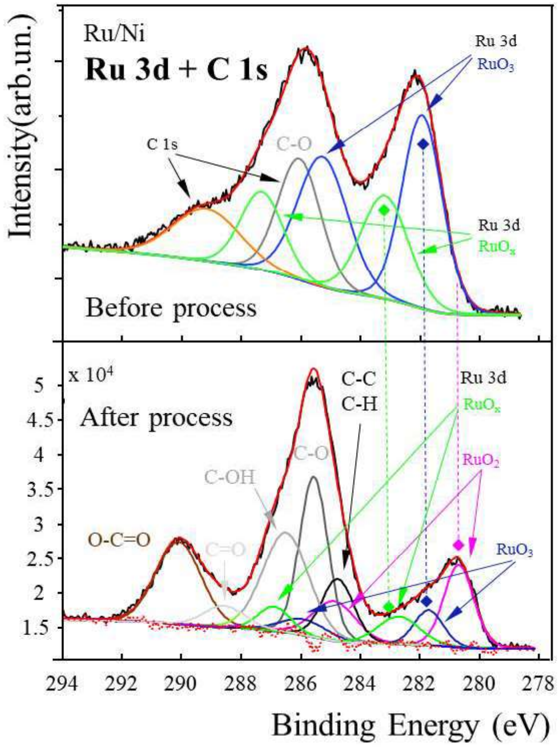
Ru/Ni
Ru 3d + C 1s
Intensity(arb.un.)
C 1s
C-O
Ru 3d
$RuO_3$
Ru 3d
$RuO_x$
Before process
x $10^4$
After process
C-C
C-H
Ru 3d
$RuO_x$
$RuO_2$
C-O
C-OH
O-C=O
C=O
$RuO_3$
5
4.5
4
3.5
3
2.5
2
1.5
294
292
290
288
286
284
282
280
278
Binding Energy (eV)

a)

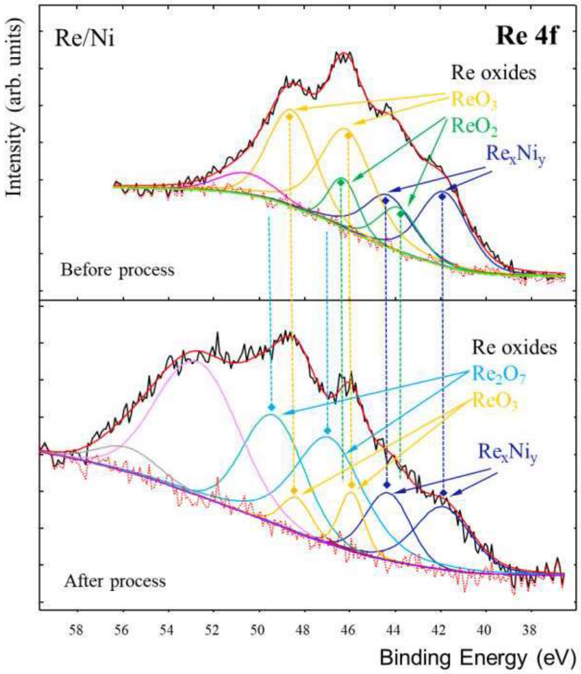
Re/Ni
Re 4f
Intensity (arb. units)
Re oxides
$ReO_3$
$ReO_2$
$Re_xNi_y$
Before process
Re oxides
$Re_2O_7$
$ReO_3$
$Re_xNi_y$
After process
58
56
54
52
50
48
46
44
42
40
38
Binding Energy (eV)

b)

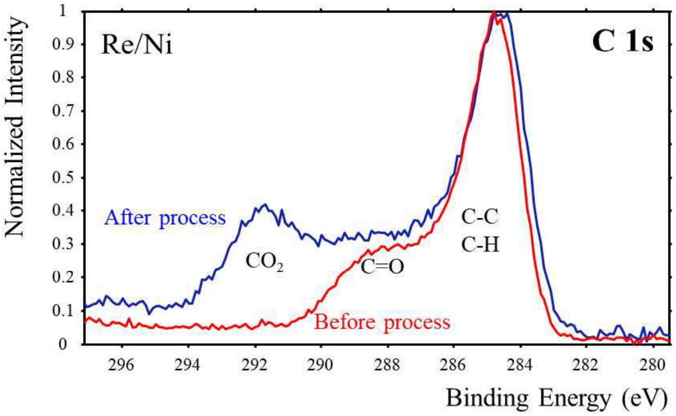

c)

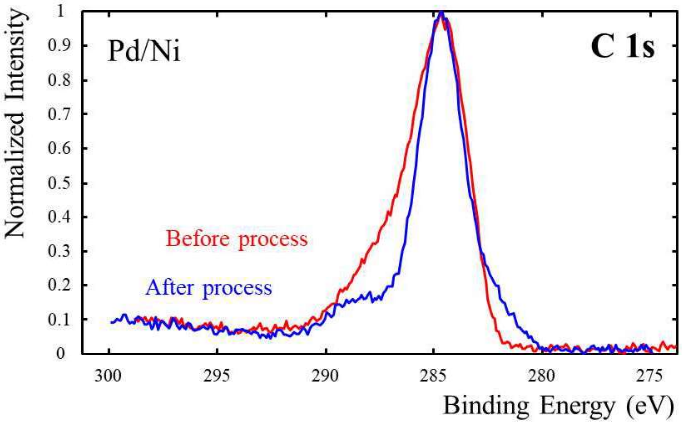

d)

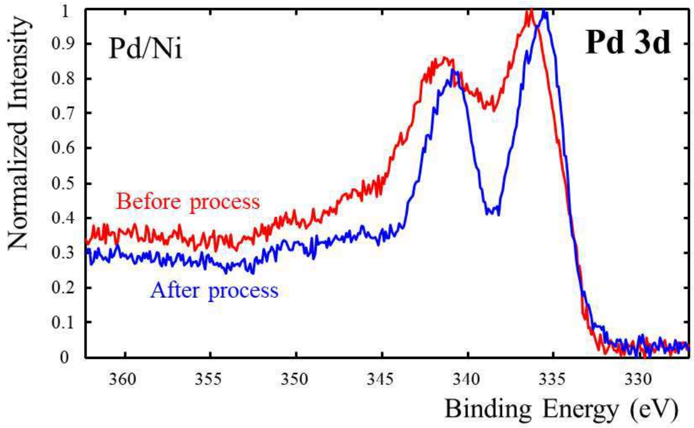

e)

**Figure S1.** Results of XPS analysis of catalysts: nRu/Ni (a), nRe/Ni (b, c) and nPd/Ni (d, e) before and after reaction

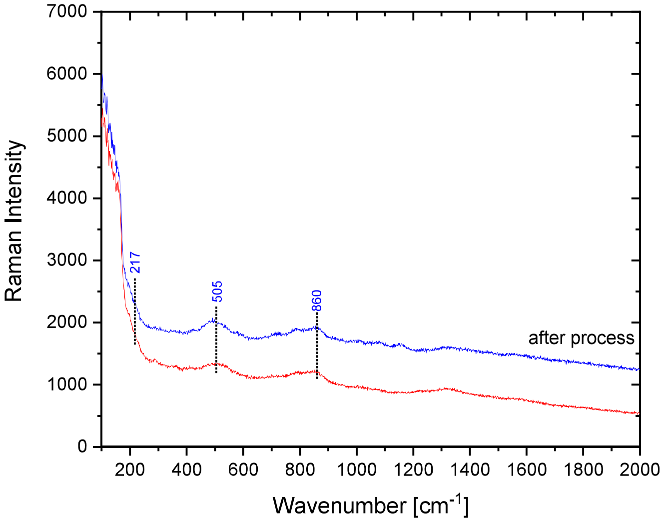

**Figure S2.** Results of Raman spectroscopy analysis of nRu/Ni catalyst before and after reaction.

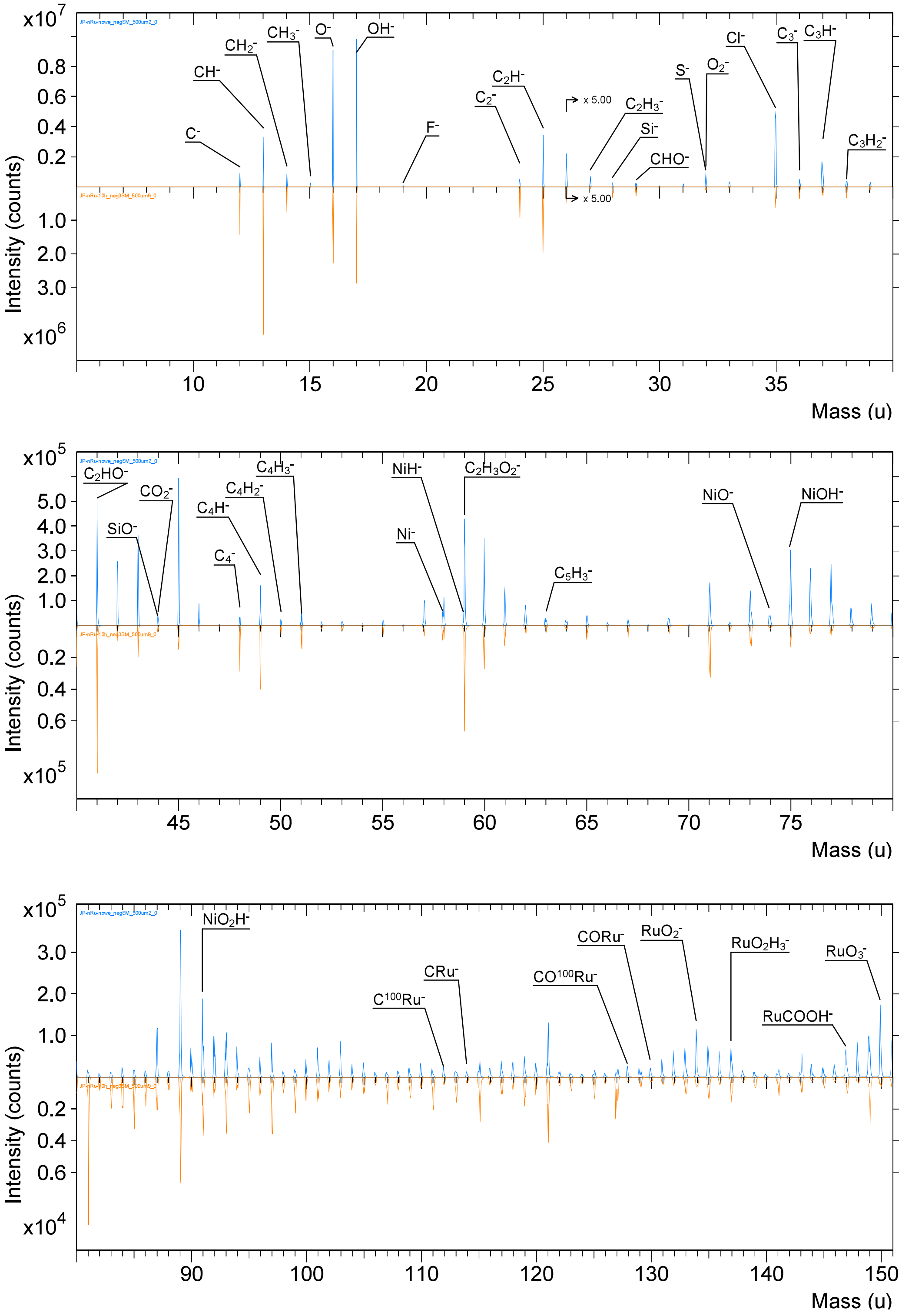

**Figure S3a.** Negative TOF-SIMS spectra obtained from sample before (blue) and after (orange) process presented in narrowed mass range (a) 5-40 u - the region form mas 24 u was magnified 5 times, (b) 40-80 u, (c) 80-150 u.

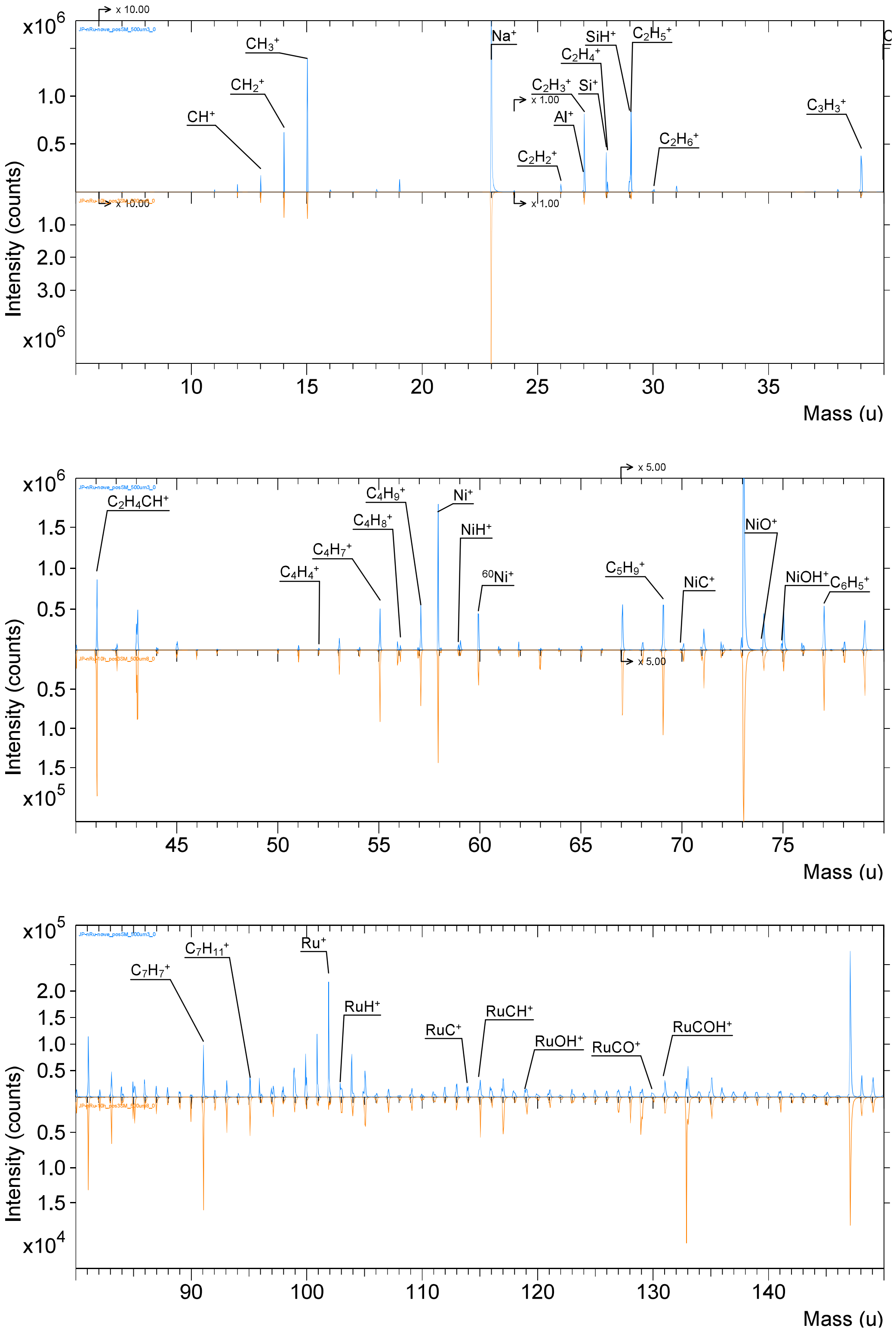

**Figure S3b.** Positive TOF-SIMS spectra obtained from sample before (blue) and after (orange) process presented in narrowed mass range (a) 5-40 u - the region form mas 5 to 24 u was magnified 10 times, above ma 24 u the spectra is presented in normal scale (b) 40-80 u, above 67 u the spectra were magnified 5 times, (c) 80-150 u.

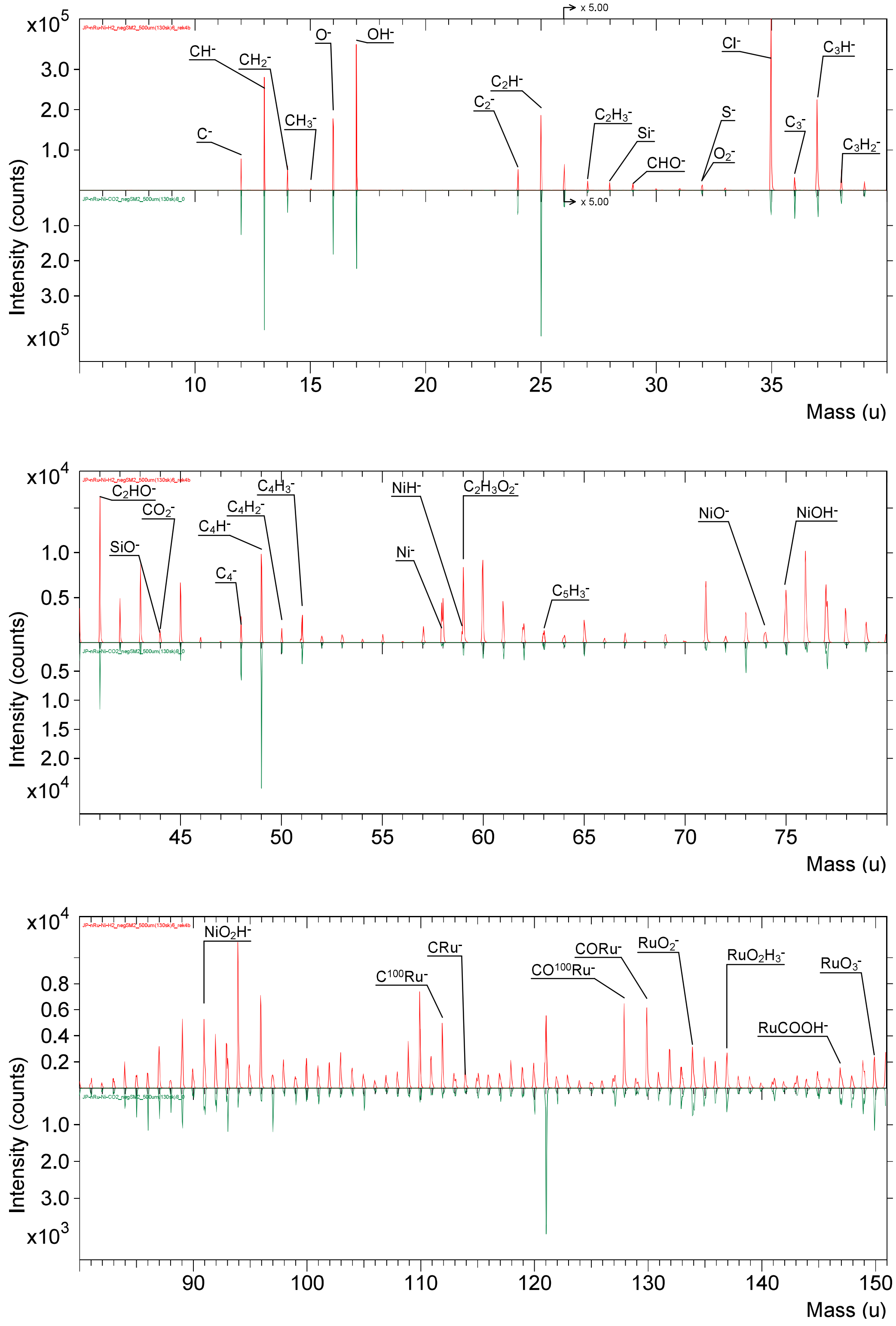

**Figure S3c.** Negative TOF-SIMS spectra obtained from sample treated with $H_2$ (red) and $CO_2$ (green) presented in narrowed mass range (a) 5-40 u - the region form mas 24 u was magnified 5 times, (b) 40-80 u, (c) 80-150 u.

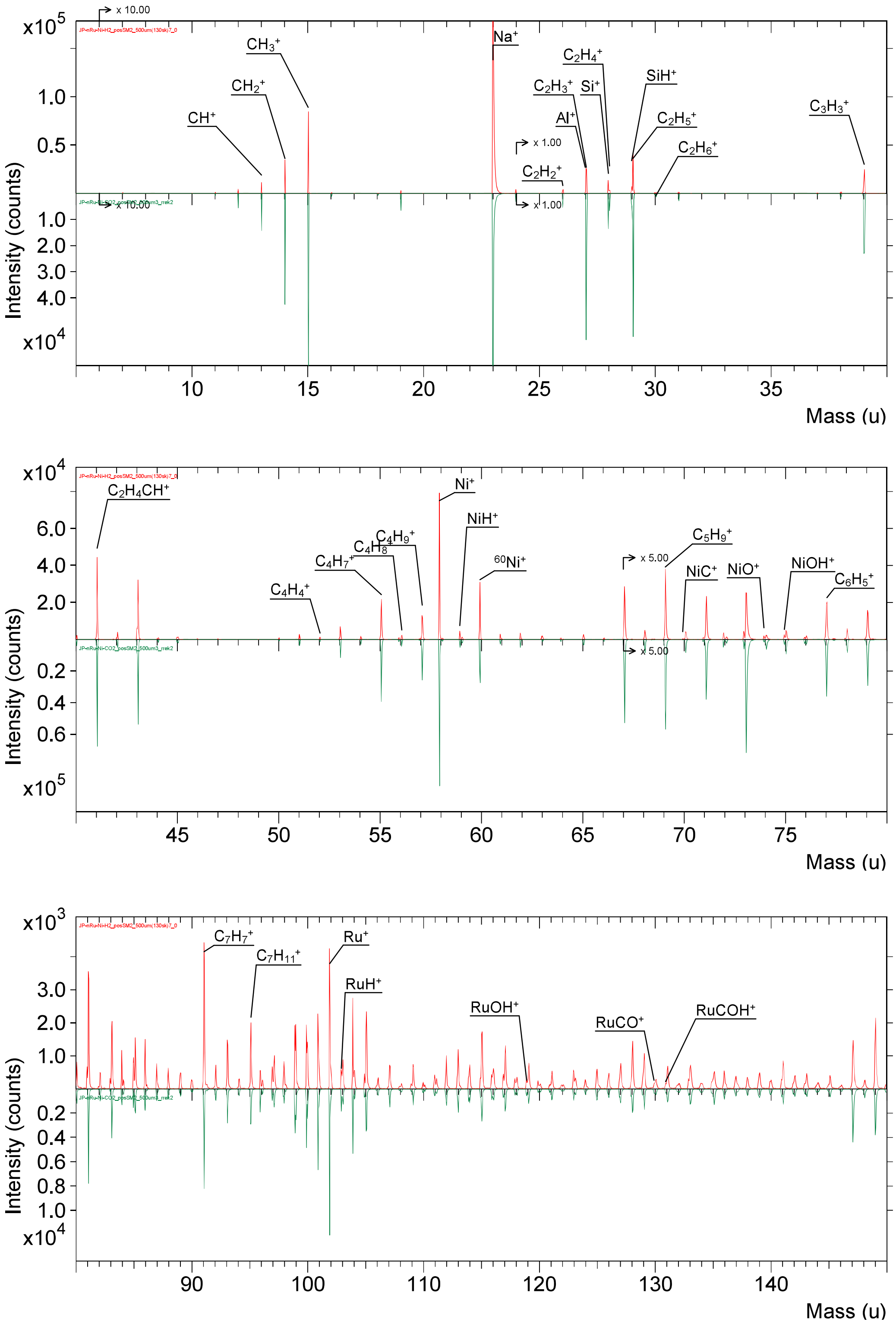

**Figure S3d.** Positive TOF-SIMS spectra obtained from sample treated with $H_2$ (red) and $CO_2$ (green) process presented in narrowed mass range (a) 5-40 u - the region form mas 5 to 24 u was magnified 10 times, above ma 24 u the spectra is presented in normal scale (b) 40-80 u, above 67 u the spectra were magnified 5 times, (c) 80-150 u.

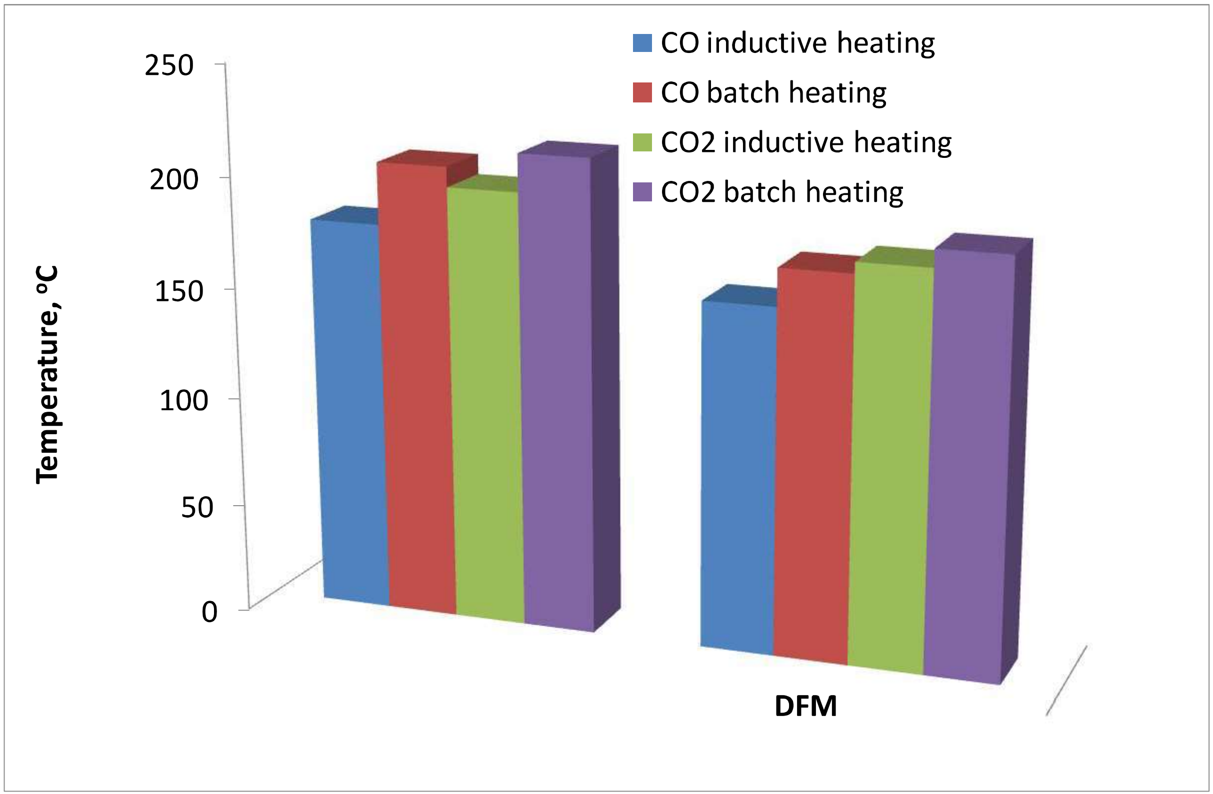

**Figure S4.** The full conversion degree of CO vs temperature with water sorption (DFM) and without water sorption (DFM unsuported system).

**Table S1** Results of EDXRF analysis of Ni supported catalysts.

| **Catalyst** | **Chemical element [wt%]** | | | **SSA[a]** |
|---|---|---|---|---|
| | **Re** | **Ru** | **Pd** | **[$m^2$/g]** |
| Ni | - | - | - | 104.8 |
| nRe/Ni | 0.18 ± 0.007 | - | - | 111.3 |
| nRu/Ni | - | 1.44 ± 0.045 | - | 129.1 |
| nPd/Ni | - | - | 0.50 ± 0.014 | 120.7 |

**Table S2** The average crystallite size and lattice parameters of investigated nanomaterials determined by XRD method.

| **Catalyst** | **Lattice parameters [Å]** | | **D [nm] Ni** | **D [nm] Pd** | **D [nm] Ru** |
|---|---|---|---|---|---|
| Ni | for Ni[a]<br>a=3.527 (±006) | - | 8 | - | - |
| nPd/Ni | for Ni[a]<br>a=3.524(±002) | for Pd[a]<br>a=4.060(±008) | 9 | 3-4 | - |
| nRu/Ni | for Ni[a]<br>a=3.526 ±0,003) | for Ru[b]<br>a=2.711(±006)<br>c=4.277(±007) | 9 | - | 4-5 |

a\ cubic, $Fm\bar{3}m$
b\ hexagonal, $P6_3/mmc$

**Table S3.** Effect of temperature and heating mode on Ru/Ni-catalysed CO and $CO_2$ methanation

CO

| No | $T_{cat}$ / °C | $\Delta$ / °C | Conv. /%[b] |
|---|---|---|---|
| 1 | -7 | 0 | 1.2$^{\text{Cyc}}$ |
| 2 | 0 | 1 | 2.9 $^{\text{Cyc}}$ |
| 3 | 27 | 0 | 16.7$^{\text{Cyc}}$ |

| | inductive heating | | | | batch heating | | |
|---|---|---|---|---|---|---|---|
| No | $T_{cat}$ / °C | $\Delta$ / °C | Conv. /%[b] | $T_{in}$ / °C | $T_{cat}$ / °C | $\Delta$ / °C | Conv. /%[b] |
| 4 | 92 | 65 | 30.1$^{\text{Con}}$ | 25 | 94 | 66 | 25.2 |
| 5 | 100 | 72 | 31.3$^{\text{Con}}$ | 25 | 100 | 71 | 26.9 |
| 6 | 130 | 103 | 49.0$^{\text{Con}}$ | 25 | 130 | 103 | 40.6 |
| 7 | 178 | 152 | 100$^{\text{Con}}$ | 25 | 206 | 181 | 100 |

$CO_2$

| No | $T_{cat}$ / °C | $\Delta$ / °C | Conv. /% |
|---|---|---|---|
| 8 | -7 | -0 | 0.0 |
| 9 | 0 | 1 | 0.0 |
| 10 | 25 | 0 | 0.0 |

| | inductive heating | | | | batch heating | | |
|---|---|---|---|---|---|---|---|
| No | $T_{cat}$ / °C | $\Delta$ / °C | Conv. /%[b] | $T_{in}$ / °C | $T_{cat}$ / °C | $\Delta$ / °C | Conv. /%[b] |
| 11 | 100 | 71 | 0.0 | 25 | 100 | 71 | 0.0 |
| 12 | 133 | 103 | 0.1 | 25 | 169 | 139 | 0.1 |
| 13 | 197 | 172 | 100 | 25 | 214 | 188 | 100 |

a/ H-heating, C-cooling; 0-without cooling or heating;

b/ Cyc- cyclic process; Cont – continuous process

**Table S4.** CO and $CO_2$ methanation with $H_2O$ removal

CO

| No | Heating/ Cooling[a] | $T_{in}$ / °C | $T_{cat}$ / °C | $T_{out}$ / °C | Conv. /%[b] | | | | |
|---|---|---|---|---|---|---|---|---|---|
| 1 | C | -7 | -7 | -7 | 0.8 | | | | |
| 2 | C | 0 | 0 | 1 | 2.1 | | | | |
| 3 | 0 | 25 | 27 | 25 | 17.9 | | | | |
| | | inductive heating | | | | batch heating | | | |
| No | Heating/ Cooling[a] | $T_{in}$ / °C | $T_{cat}$ / °C | $T_{out}$ / °C | Conv. /%[b] | $T_{in}$ / °C | $T_{cat}$ / °C | $T_{out}$ / °C | Conv. /%[b] |
| 4 | H | 25 | 92 | 90 | 35.3 | 25 | 94 | 91 | 27.4 |
| 5 | H | 25 | 100 | 97 | 37.2 | 25 | 100 | 96 | 29.0 |
| 6 | H | 25 | 130 | 128 | 58.8 | 25 | 130 | 128 | 44.1 |
| 7 | H | 25 | 156 | 156 | 100 | 25 | 173 | 172 | 100 |

$CO_2$

| No | Heating/ Cooling[a] | $T_{in}$ / °C | $T_{cat}$ / °C | $T_{out}$ / °C | Conv. /% | | | | |
|---|---|---|---|---|---|---|---|---|---|
| 8 | C | -7 | -7 | -7 | 0.0 | | | | |
| 9 | C | 0 | 0 | 1 | 0.0 | | | | |
| 10 | 0 | 25 | 25 | 25 | 0.0 | | | | |
| | | inductive heating | | | | batch heating | | | |
| No | Heating/ Cooling[a] | $T_{in}$ / °C | $T_{cat}$ / °C | $T_{out}$ / °C | Conv. /%[b] | $T_{in}$ / °C | $T_{cat}$ / °C | $T_{out}$ / °C | Conv. /%[b] |
| 11 | H | 25 | 100 | 96 | 0.0 | 25 | 100 | 96 | 0.0 |
| 12 | H | 25 | 130 | 127 | 0.1 | 25 | 147 | 143 | 0.1 |
| 13 | H | 25 | 178 | 178 | 100 | 25 | 186 | 185 | 100 |

a/ H-heating, C-cooling; 0-without cooling or heating;

b/ Cyc- cyclic process; Cont – continuous process

**Table S5.** Effect of temperature and heating mode on Re/Ni-catalysed CO and $CO_2$ methanation

CO

| No | $T_{cat}$ / °C | Δ / °C | Conv. /%[b] |
|---|---|---|---|
| 1 | -7 | 0 | 0.0 |
| 2 | 0 | 0 | 0.0 |
| 3 | 27 | 0 | 0.0 |

|  | inductive heating |  |  |  | batch heating |  |  |
|---|---|---|---|---|---|---|---|
| No | $T_{cat}$ / °C | Δ / °C | Conv. /%[b] | $T_{in}$ / °C | $T_{cat}$ / °C | Δ / °C | Conv. /%[b] |
| 4 | 95 | 67 | $12.3^{Con}$ | 25 | 94 | 66 | 9.5 |
| 5 | 100 | 74 | $14.0^{Con}$ | 25 | 100 | 73 | 10.9 |
| 6 | 130 | 104 | $25.1^{Con}$ | 25 | 130 | 102 | 19.2 |
| 7 | 298 | 271 | $100.0^{Con}$ | 25 | 310 | 285 | 100.0 |

$CO_2$

| No | $T_{cat}$ / °C | Δ / °C | Conv. /% |
|---|---|---|---|
| 8 | -7 | -0 | 0.0 |
| 9 | 0 | 0 | 0.0 |
| 10 | 25 | 0 | 0.0 |

|  | inductive heating |  |  |  | batch heating |  |  |
|---|---|---|---|---|---|---|---|
| No | $T_{cat}$ / °C | Δ / °C | Conv. /%[b] | $T_{in}$ / °C | $T_{cat}$ / °C | Δ / °C | Conv. /%[b] |
| 11 | 100 | 74 | 0.0 | 25 | 100 | 73 | 0.0 |
| 12 | 182 | 155 | 0.1 | 25 | 193 | 166 | 0.1 |
| 13 | 319 | 292 | 100.0 | 25 | 331 | 305 | 100.0 |

a/ H-heating, C-cooling; 0-without cooling or heating;

b/ Cyc- cyclic process; Cont – continuous process

### Preparation of $Ru_{NPs}$ (Pd, Re)$_{NPs}$ on Ni

In typical procedure we prepared $Ru_{NPs}$ on silica as an auxiliary source of nanoparticles. Silica was prepared using the Stöber method [32] with tetraethyl orthosilicate (TEOS), which was added to a mixture of ethanol and an aqueous ammonia solution. After silica separation, a solution of a ruthenium precursor ($RuCl_3$) was added. The mixture was sonicated, then concentrated, dried and reduced under hydrogen at 500°C. In a typical procedure, 800 mL of anhydrous ethanol and 135 mL of 25 wt.% solution of ammonia were mixed with 78 mL of deionized water. After 10 min of stirring, 60 mL of tetraethyl orthosilicate was added to the reaction mixture, which was next stirred for 3 h at room temperature. The colloidal silica suspension that was obtained was centrifuged, washed to neutral pH (deionized water) and suspended in deionized water (20 mL) in an ultrasound bath and stirred for 90 min. A solution containing the ruthenium precursor (445 mg ruthenium(III) chloride hydrate for 1.0% $Ru/SiO_2$) in deionized water (30 mL) was added dropwise into the colloidal silica suspension and mixed in an ultrasound bath for 30 min. Next, it was dried to a constant weight at approx. 90°C, ground and sieved. The reduction was conducted in an oven under hydrogen at 500°C for 4 h. A bimetallic $Ru_{NPs}$/Ni catalyst was prepared using a novel facile approach that involved the transfer of the nanoparticles from the intermediate carrier, i.e. $SiO_2$ to the target carrier. The general method includes several steps. The target carrier, i.e. Ni, (0.99 g) and $Ru_{NPs}$ of a low polydispersity were deposited on the intermediate carrier i.e. 1.0% $Ru_{NPs}/SiO_2$, (1.00 g), Then this was suspended in deionized water (100 mL) under mechanical stirring and sonication. After 10 minutes of vigorous stirring, sodium hydroxide (40 mL 40% w/w) was added to the suspension and stirring was continued for 4 h at 80°C, whereupon the suspension was allowed to stand for about 18 h until the suspended solids sedimented. The suspension was centrifuged and the supernatant was decanted, and then the precipitate was washed in deionized water and centrifuged again to achieve a neutral pH of the supernatant. The precipitate was washed with deionized water once again, centrifuged and the supernatant was removed. The catalyst that was obtained was dried in an electric dryer to a constant weight at 110°C. The same method was used to prepare $Pd_{NPs}$ and $Re_{NPs}$ supported on Ni.

## Methods of catalyst characterization

The chemical analysis was performed using energy-dispersive X-ray fluorescence (EDXRF) spectrometer - Epsilon 3 (Panalytical, Almelo, The Netherlands) with a Rh target X-ray tube operated at max. voltage of 30 keV and max. power of 9W. The spectrometer is equipped with thermoelectrically cooled silicon drift detector (SDD) with 8μm Be window and resolution of 135 eV at 5.9 keV. The quantitative analysis was performed using Omnian software based on fundamental parameter method and following measurement conditions: 5 kV, 300 s counting time, helium atmosphere for Si and P determination; 12 kV, 300 s counting time, helium atmosphere, 50 μm Al primary beam filter for Ca; 20 kV, 120 s counting time, air atmosphere, 200 μm Al primary beam filter for Fe; and 30 kV, 120 s counting time, air atmosphere, 100 μm Ag primary beam filter for Ni, Zn and Ru. The current of the X-ray tube were fixed to not exceed dead-time loss of ca. 50%.

The transmission electron microscopy (TEM) observations were performed using a JEOL high resolution (HRTEM) JEM 3010 microscope working at 300 kV accelerating voltage and equipped with Gatan 2k×2k Orius$_{TM}$ 833SC200D CCD camera and EDS detector. The samples were suspended in isopropanol and the resulted materials were deposited on Cu grid coated with amorphous carbon film standardized for TEM observations.

The structural features of the catalysts were studied by X-ray diffraction technique (XRD). The experiments were carried out on a high-resolution PANalytical Empyrean diffractometer with Cu $K_{\alpha}$ radiation (40kV, 30mA) equipped with a PIXcel detector. Data was collected in the 10°–140° $2\theta$ range with 0.0131° step. The phase analysis was performed by the "X'Pert High Score Plus" computer program and with the data from ICDD PDF-4 database.

The Ni based bimetallic systems were examined by X-ray photoelectron spectroscopy (XPS) with the use of Physical Electronics PHI 5700 spectrometer. Monochromatic AlKα x-ray radiation (hν = 1486.7 eV) was used to obtain the photoelectron spectra of core levels of particular elements. The structure of the obtained XPS multiplets was analyzed with the use of Multipak v. 9.0softwarefrom Physical Electronics.

3Flex apparatus, produced by Micromeritics, USA, was employed to determine the $N_2$ adsorption isotherm at 77 K in the range of 0.05 to 0.3 relative pressure in order to calculate the BET surface area. Prior to the measurement, the sample was degassed under vacuum at 350°C for 5 h.

Raman spectra in 50 – 2000 $cm^{-1}$ range were collected using XploRA™ PLUS Confocal Raman Spectrometer from Horiba Jobin Yvon company. The spectra were collected using an air-cooled solid-state laser (785 nm wavelength) and 1024×256 TE air-cooled scientific CCD detector. Measurements were conducted with 1200 lines·$mm^{-1}$ grating. The microscope used a 100× objective and a confocal pinhole of 500 µm. The Raman spectrometer was calibrated using a silicon wafer. The spectra were collected by 5 scans with an integration time of 200 s. Raman spectroscopy has been used to study the material before and after the reaction. Fig. S3. shows that in both samples spectra bands at 500 $cm^{-1}$ and 860 $cm^{-1}$ are observed. Other spectral bands were not observed. The both bands can be attributed to the nickel oxide present at the particles surface. The band at 505 $cm^{-1}$ corresponds to the Ni – O stretching mode and is due to the photon excitement in nanosized NiO. The band around at 860 $cm^{-1}$ is due to two-phonon excitation. The intensity of one-phonon scattering increases significantly when NiO is defect-rich or due to the surface effect what can explain that other NiO bands were not observed.

## TEM microscopy of the catalyst

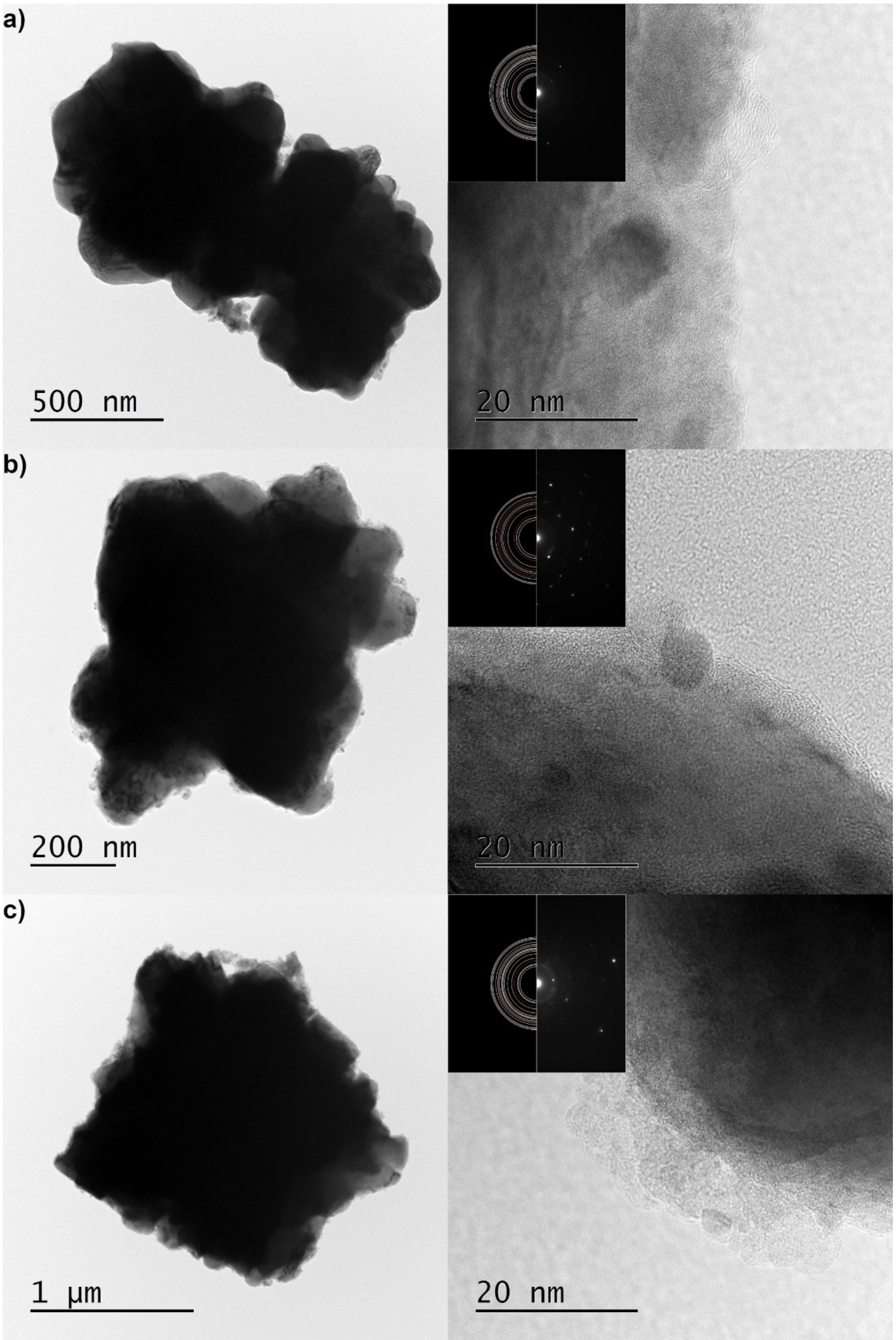

**Figure S5.** TEM micrographs showing a) Re, b) Pd and c) Ru nano-particles on the surface of the Ni microparticles. Left part of the figure shows images recorded in the bright field whereas the right part shows high-resolution image. Insight show electron diffraction patterns with corresponding theoretical rings white for nanoparticle material, red for Ni.

The transmission electron microscopy (TEM) observations were performed using JEOL JEM-3010 high-resolution (HR-TEM) machine working with 300 kV acceleration voltage and equipped with a Gatan 2k × 2k Orius™ 833 SC200D CCD camera. Samples were solubilized in isopropanol and deposited on the Cu grid coted with a thin layer of amorphous carbon, standardized for the TEM observations.

The performed TEM observations showed microscale Ni particles with remaining of the amorphous silica. Performed high-resolution images revealed the presence of Re, Pd and Ru nano-particles arranged individually and as conglomerates on the surface of the Ni particles.

## The analysis of chemical states of Ni by XPS

The analysis of chemical states of Ni (see S1(a) the deconvoluted high resolution XPS spectra of Ni2p3/2) before and after carbon (di)oxide methanation indicate presence of NiO [1], recognized also in Ru-Ni/$Al_2O_3$ system [2] and Ni2O3 with a binding energy as in [3].

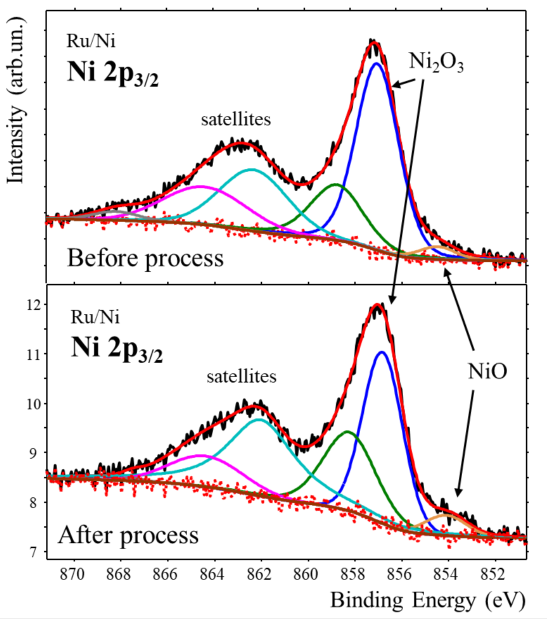

**Figure S6.** XPS spectra of the Ru/Ni catalyst before and after reaction

Unlike in other studies of Ru-Ni nanostructured systems [2,4] nickel in the metallic form ($Ni^0$) was not observed. A slight increase of NiO oxide was observed after the process would suggest partial $Ni^{2+}$ to $Ni^{3+}$ valence transition. The most probable mechanism that leads for such transition would take place through the presence of hydrogen (most likely hydrogen in $Ni(OH)_2$, not detected with the use of the XPS but suspected to be present by detection of the NiOH- ions in the TOF-SIMS mass spectra. The analysis of the changes of the intensity ratio indicate reduction of the $NiOH^-$ ions in comparison to $NiO^-$ (see Fig S3a at mass 75 Da). The detection limits and surface sensitivity of TOF-SIMS mass spectroscopy are higher than XPS, thus the mass spectra were additionally used for the observation of the catalyst surface species.

## Mass balance for CO and $CO_2$ methanation

$CO_2$ methanation (full conversion; temp. 197ºC):
Inlet gas flow 3dm3/h: 20%v $CO_2$ + 80%v $H_2$
$H_2O$ adsorption in molecular sieve 4A, mass increase after 0,5h Δm=0,494g (theoretical Δm=0,482g)
Outlet gas flow (measured after steam adsorption) ~0,65dm3/h

CO methanation (full conversion; temp. 178 ºC):
Inlet gas flow 3dm3/h: 25%v CO + 75%v $H_2$
$H_2O$ adsorption in molecular sieve 4A, mass increase after 0,5h Δm=0,312g (theoretical Δm=0,301g)
Outlet gas flow (measured after steam adsorption) ~0,75dm3/h

## Selected literature references for CO methanation

A variety of systems were described for CO methanation. The usual temperatures needed to operate these systems range 270-400ºC (for the extensive literature survey see Supporting Information).

[B] J. Gao, C. Jia, M. Zhang, F. Gu, G. Xu, F. Su, Effect of nickel nanoparticle size in Ni/ α-$Al_2O_3$ on CO methanation reaction for the production of synthetic natural gas, Catal. Sci. Technol. 3 (2013) 2009.
[C] G. Jin, F. Gu, Q. Liu, X. Wang, L. Jia, G. Xu, Z. Zhong, F. Su, Highly stable Ni/SiC catalyst modified by $Al_2O_3$ for CO methanation reaction, RSC Adv. 6 (2016) 9631–9639.
[D] Q. Liu, J. Gao, F. Gu, X. Lu, Y. Liu, H. Li, Z. Zhong, B. Liu, G. Xu, F. Su, One-pot synthesis of ordered mesoporous Ni–V–Al catalysts for CO methanation, J. Catal. 326 (2015) 127–138.
[E] M. Tao, X. Meng, Y. Lv, Z. Bian, Z. Xin, Effect of impregnation solvent on Ni dispersion and catalytic properties of Ni/SBA-15 for CO methanation reaction, Fuel 165 (2016) 289–297.
[F] C. Yuan, N. Yao, X. Wang, J. Wang, D. Lv, X. Li, The $SiO_2$ supported bimetallic Ni–Ru particles: a good sulfur-tolerant catalyst for methanation reaction, Chem. Eng. J. 260 (2015) 1–10.
[G] J. Zhang, Z. Xin, X. Meng, Y. Lv, M. Tao, Effect of $MoO_3$ on the heat resistant performances of nickel based MCM-41 methanation catalysts, Fuel 116 (2014) 25–33.
[H] J. Gao, C. Jia, J. Li, M. Zhang, F. Gu, G. Xu, Z. Zhong, F. Su, Ni/$Al_2O_3$ catalysts for CO methanation: effect of Al2O3 supports calcined at different temperatures, J. Energy Chem. 22 (2013) 919–927.
[I] J. Liu, W. Shen, D. Cui, J. Yu, F. Su, G. Xu, Syngas methanation for substitute natural gas over Ni–Mg/$Al_2O_3$ catalyst in fixed and fluidized bed reactors, Catal. Commun. 38 (2013) 35–39.
[J] P. Liu, B. Zhao, S. Li, H. Shi, M. Ma, J. Lu, F. Yang, X. Deng, X. Jia, X. Ma, X. Yan, Influence of the Microstructure of Ni–Co Bimetallic Catalyst on CO Methanation, Ind. Eng. Chem. Res. 2020, 59, 5, 1845-1854.
[K] S. Li, D. Gong, H. Tang, Z. Ma, Z. Liu, Y. Liu, Preparation of bimetallic Ni@Ru nanoparticles supported on $SiO_2$ and their catalytic performance for CO methanation, Chem. Eng. J. 2017, 334, 2167.
[L] Y. Liu, W. Sheng, Z. Hou, Y. Zhang, Homogeneous and highly dispersed Ni–Ru on a silica support as an effective CO methanation catalyst, RSC Adv., 2018, 8, 2123–2131